

Binary Transition Metal Dinitrogen Complexes. I. Matrix Infrared and Raman Spectra, Structure, and Bonding of $\text{Ni}(\text{N}_2)_n$ and $\text{Pd}(\text{N}_2)_m$ ($n = 1-4$ and $m = 1-3$)

H. Huber, E. P. Kundig, M. Moskovits, and G. A. Ozin*

Contribution from the Lash Miller Chemical Laboratories and Erindale College,
University of Toronto, Toronto, Canada. Received July 6, 1972

Abstract: The products of the cocondensation reactions of Ni and Pd atoms with N_2 at 4.2–10°K are investigated by matrix isolation infrared and Raman spectroscopy and are shown to be binary dinitrogen complexes of the form $\text{Ni}(\text{N}_2)_n$ and $\text{Pd}(\text{N}_2)_m$. Examination of the reaction products in pure $^{14}\text{N}_2$, in $^{14}\text{N}_2/^{15}\text{N}_2$, and in dilute $\text{Ar}/^{14}\text{N}_2$, $\text{Ar}/^{14}\text{N}_2/^{15}\text{N}_2$, and $\text{Ar}/^{14}\text{N}/^{15}\text{N}$ matrices establishes the stoichiometries of the complexes to be respectively $n = 1-4$ and $m = 1-3$. Structural assignments can be made for most of the complexes on the basis of infrared and Raman activities and are found to be similar to the analogous carbonyls. Isotopic frequencies and integrated infrared absorption intensities, computed for the NN stretching modes of the individual dinitrogen complexes on the basis of the Cotton-Kraihanzel force field approximation and on isotopic intensity sum rules, are found to be in close agreement with the observed values. $\text{Ni}(\text{N}_2)_4$ in argon is a regular tetrahedral molecule with "end on bonded" dinitrogen. In nitrogen, however, it is slightly distorted. Calculations show that a substitutional site symmetry of C_2 for $\text{Ni}(\text{N}_2)_4$ satisfactorily accounts for all of the spectral lines observed for the complex in nitrogen.

The two isoelectronic molecules nitrogen and carbon monoxide have long been recognized to exhibit similar properties under many circumstances, for example, their crystal structures at low temperatures are isomorphous.^{1,2} More pointedly, the metal-ligand bonding in coordination complexes where nitrogen bonds as a neutral ligand appears to be very similar to that found in metal carbonyls.³

Of the two, N_2 and CO , the former has evoked the greater interest in recent years because it has proved possible to "fix" atmospheric nitrogen in several inorganic systems⁴ in a way which parallels the biological conversion of ambient N_2 to NH_3 by nitrogen fixing bacteria. Despite vigorous research in this area, binary metal dinitrogen complexes analogous to the metal carbonyls have not been reported with one exception⁵ which we discuss below.

In this paper we describe the synthesis and characterization of the binary nickel and palladium dinitrogen compounds in low temperature matrices. These investigations follow logically our work with the intermediate carbonyls of the same metals.⁶ The potential existence of these dinitrogen compounds was often foreshadowed during our experiments with carbonyls by the presence of "impurity" lines which we were forced to conclude belonged to the dinitrogen species. Recently, too, Burdett and Turner⁵ have reported preliminary infrared data for the Ni/N_2 reaction in low temperature matrices which indicated that nickel dinitrogen complexes are capable of existence under those conditions. As part of the present study, we had to perform Ni/N_2 experiments similar to theirs. Our results, however, differ markedly with theirs in several respects, and necessitate a reappraisal of their data.

Briefly, our technique involves the cocondensation of

metal atoms with nitrogen or nitrogen in argon at 4.2–10°, followed by spectroscopic examination. Matrix infrared and matrix Raman were both used. The latter carries with it the possibility of performing matrix depolarization measurements,⁷ thereby identifying the totally symmetric vibrational modes.

Mixed isotopic matrix gases were also used to help establish the coordination number of the reaction products under different degrees of matrix dilution. Warm-up experiments were performed which aid in the assignment of the spectral lines to the several species which could be present in the matrix.

Experimental Section

Monatomic Ni and Pd vapors were generated by directly heating a thin (0.008 in.) ribbon filament of the metal with AC. The nickel (99.99%) and palladium (99.99%) were supplied by McKay Inc., New York, N. Y. Research grade $^{14}\text{N}_2$ (99.99%) and Ar (99.99%) were supplied by Matheson. Isotopically enriched $^{15}\text{N}_2$ (99.5%) was supplied by Prochem. A mixture of $^{14}\text{N}_2$, $^{15}\text{N}^{14}\text{N}$, and $^{15}\text{N}_2$ in the ratio 1:2:1 was prepared by conventional techniques.

The furnace used for the evaporation of the metals has been described previously.⁶ The rate of metal atom depositions was continuously monitored using a quartz crystal microbalance.⁸ The deposition rate was set such that the probability that a metal atom had another metal atom as a nearest neighbor in either the N_2 or Ar fcc lattice was approximately 1 in 10^3 . Matrix gas flows, controlled by a calibrated micrometer needle valve, were usually in the range 2–8 mmol/hr. In the infrared experiments matrices were deposited on a cryotip cooled to 10°K by means of an Air Products Displex closed cycle helium refrigerator. Spectra were recorded on a Perkin-Elmer 180 spectrophotometer. In the Raman experiments the matrices were deposited on a liquid helium cooled (4.2°K) cryotip. Spectra were recorded on a Spex Model 1401 Raman spectrophotometer using Carson argon ion 4880- and 5145-Å laser excitation.

Results and Discussion

Nickel-Nitrogen System. When nickel atoms are cocondensed with a 1:10 mixture of $^{14}\text{N}_2$ in Ar, the matrix infrared spectrum shown in Figure 1 and Table I is obtained. The spectrum shows three strong lines at 2088, 2106, and 2134 cm^{-1} and a weak line at 2174

(1) R. W. G. Wyckoff, "Crystal Structures," Vol. 7, Interscience, New York, N. Y., p 29.

(2) Reference 1, p 185.

(3) A. D. Allen and F. Bottomly, *Accounts Chem. Res.*, **1**, 360 (1968).

(4) E. E. Van Tamelen, *ibid.*, **3**, 361 (1970).

(5) J. K. Burdett and J. J. Turner, *Chem. Commun.*, 885 (1971).

(6) H. Huber, E. P. Kundig, M. Moskovits, and G. A. Ozin, *Nature Phys. Science*, **235**, 98 (1972); *J. Mol. Struct.*, in press; *Can. J. Chem.*, in press.

(7) H. Huber, G. A. Ozin, and A. Vander Voet, *Nature Phys. Sci.*, **232**, 166 (1971).

(8) M. Moskovits and G. A. Ozin, *Appl. Spectrosc.*, **26**, 481 (1972).

Table I. Matrix Infrared and Raman Spectra of the Products of the Cocondensation Reaction of Ni Atoms with Dilute $^{14}\text{N}_2/\text{Ar}$ Mixtures

Infrared $\text{N}_2:\text{Ar}$ 1:10		Raman $\text{N}_2:\text{Ar}$ 1:10		Infrared $\text{N}_2:\text{Ar}$ 1:1000		Assignment
10°K after deposition	10°K after diffusion at 36°K	10°K after deposition	10°K after diffusion at 30°K	10°K after deposition	10°K after diffusion at 20°K	
		2246	2246			$\text{Ni}(\text{N}_2)_4$
		2232				$\text{Ni}(\text{N}_2)_3$
		2187				$\text{Ni}(\text{N}_2)_3$
2174	2174	2174	2174		2175	$\text{Ni}(\text{N}_2)_4$
2134					2137	$\text{Ni}(\text{N}_2)_3$
2106 ^a					2104	$\text{Ni}(\text{N}_2)_2$
2088		2088		2089	2089	$\text{Ni}(\text{N}_2)$

^a Matrix splitting observed for this line at 2099 cm^{-1} (confirmed by annealing and dilution experiments).

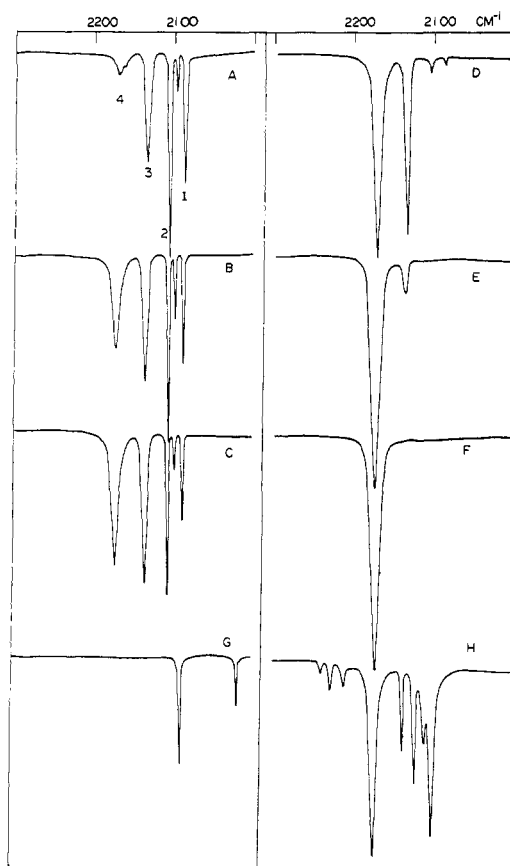


Figure 1. The matrix infrared spectra of the cocondensation reaction of Ni atoms with (A) a $^{14}\text{N}_2:\text{Ar} = 1:10$ mixture at 10°K, (B-F) after successive diffusion controlled warm-up experiments at 20, 20, 25, 30, and 35°K and then re-cooled to 10°K, (G) a $^{14}\text{N}_2:^{15}\text{N}_2:\text{Ar} = 1:1:2000$ mixture at 10°K, (H) a $^{14}\text{N}_2:^{15}\text{N}_2:\text{Ar} = 1:1:20$ mixture deposited at 10°K, allowed to diffuse at 35°K and re-cooled to 10°K.

cm^{-1} . Upon warmup these grow and decay in strength at different rates (Figure 2) to yield finally a one line (2174 cm^{-1}) spectrum as shown in Figure 1F. A *prima facie* interpretation suggests, therefore, that there are four Ni/N_2 species in the matrix when deposited. One of these (absorbing at 2174 cm^{-1}) is overwhelmingly more stable than the rest. The results of the analogous experiment using a 1:1:20, $^{14}\text{N}_2/^{15}\text{N}_2/\text{Ar}$ are shown in Figure 3. After warmup the eight-line spectrum shown in Figures 1H and 3F is obtained. That is the one line at 2174 cm^{-1} becomes eight lines in a mixed isotope

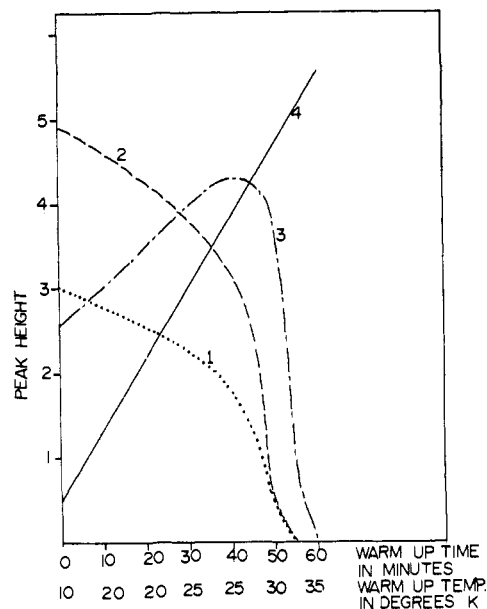


Figure 2. Graphical representation of the infrared absorption intensities of the $^{14}\text{N}_2:\text{Ar} = 1:10$, during diffusion controlled warm up in the temperature range 10–35°K.

matrix. This experiment indicates, therefore, that the stable Ni/N_2 species in the Ar matrix is $\text{Ni}(\text{N}_2)_4$. The position of the lines and the intensities (see Table I) suggest, moreover, the symmetry to be T_d . Details of the intensity and frequency calculations are given below. A matrix Raman experiment using a 1:10 $^{14}\text{N}_2/\text{Ar}$ matrix gas gave, after warmup, a result (Figure 4B) compatible with our assignment, namely one depolarized line at 2174 cm^{-1} coincident with the one line in the ir and one polarized line at 2246 cm^{-1} coincident with the calculated position of the A_1 using “Cotton-Kraihanzel” force constants⁹ obtained from the mixed isotope experiment (Table I).

Ni/N_2 Intermediate Species. NiN_2 . Returning to Figure 1, having determined that the absorption at 2174 cm^{-1} belongs to the species $\text{Ni}(\text{N}_2)_4$, it is reasonable to assume that the other three absorptions belong to the species $\text{Ni}(\text{N}_2)_x$ where $x = 1, 2, 3$.

To facilitate the assignment, nickel vapor was co-condensed with a $^{14}\text{N}_2/\text{Ar}$, 1:1000 mixture. At such a low N_2 concentration only the mononitrogen species

(9) F. A. Cotton and C. S. Kraihanzel, *J. Amer. Chem. Soc.*, **84**, 4432 (1962).

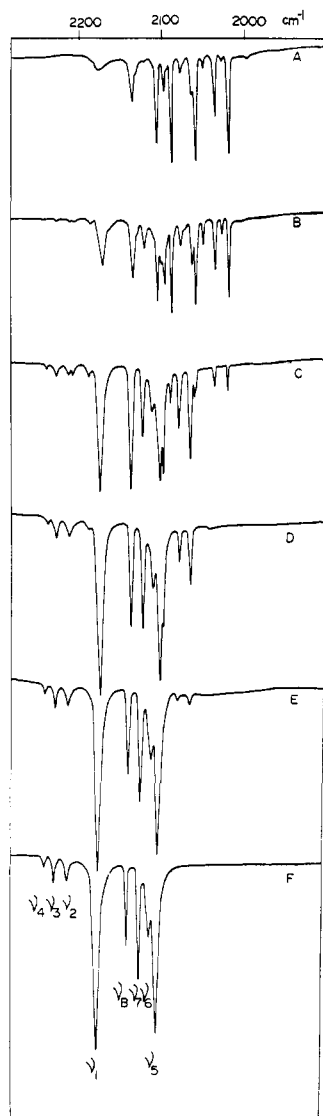


Figure 3. The matrix infrared spectrum of the cocondensation reaction of Ni atoms with (A) a $^{14}\text{N}_2$: $^{16}\text{N}_2$:Ar = 1:1:20 mixture at 10°K, (B–F) after successive diffusion-controlled warm-up experiments at 20, 20, 25, 30, and 35°K and then recooled to 10°K.

is expected to be formed and indeed only one line at 2088 cm^{-1} is observed. A mixed isotope experiment using $^{14}\text{N}_2$ / $^{15}\text{N}_2$ /Ar in the ratio 2:1:2000 gave a two line spectrum (Figure 1G) strongly suggesting that the line at 2089.9 cm^{-1} belongs to Ni($^{14}\text{N}_2$) and that at 2020.6 cm^{-1} to Ni($^{15}\text{N}_2$).

When Ni vapor was cocondensed with a 3:2:1:4000 mixture of $^{14}\text{N}_2$ / $^{14}\text{N}^{15}\text{N}$ / $^{15}\text{N}_2$ /Ar the spectrum shown in Figure 5 is obtained. The doublet at 2053.6 and 2057.4 cm^{-1} which, by a process of elimination, must belong to the Ni/ $^{14}\text{N}^{15}\text{N}$ system, is clearly visible, indicating that the nitrogen in NiN₂ is "end-on" bonded (*i.e.*, that the lines at 2053.6 and 2057.4 cm^{-1} belong to Ni $^{14}\text{N}^{15}\text{N}$ and Ni $^{15}\text{N}^{14}\text{N}$, respectively) rather than "side on" bonded since in the latter case only a single line would have been observed.

Ni(N₂)₂ and Ni(N₂)₃. The matrix Raman spectrum obtained with $^{14}\text{N}_2$ /Ar = 1:10 shown in Figure 4A shows five lines at 2246, 2232, 2187, 2174, and 2088 cm^{-1} . The bands at 2246 and 2174 cm^{-1} have already been accounted for as belonging to Ni(N₂)₄ while that at 2088 cm^{-1} belongs to NiN₂. Upon warmup the lines

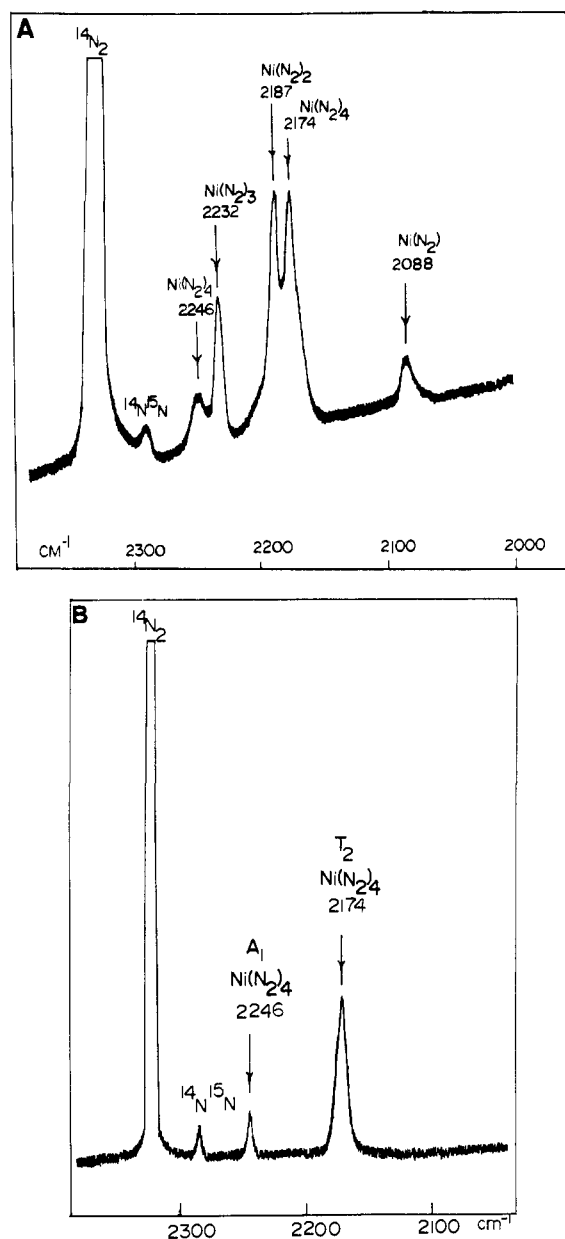


Figure 4. The matrix Raman spectra of the cocondensation reaction of Ni atoms with (A) a $^{14}\text{N}_2$:Ar = 1:10 mixture at 4.2°K, (B) after diffusion controlled warm up at 35°K.

at 2232 and 2187 cm^{-1} behave in a similar fashion to the bands at 2134 and 2106 cm^{-1} , respectively, observed in the analogous ir experiment.

From the progress and results of the warmup experiments, the lines at 2134 (ir) and 2232 (R) cm^{-1} are assigned to Ni(N₂)₃ while those at 2106 (ir) and 2187 (R) cm^{-1} are assigned to Ni(N₂)₂.

The "mutual exclusion" rule seems to be operating for the Ni(N₂)₂ molecule implying that its structure has $D_{\infty h}$ symmetry, while the absence of the line at 2232 cm^{-1} in the ir spectrum of Ni(N₂)₃ implies that it has D_{3h} symmetry.

Nickel-Pure Nitrogen System. When nickel atoms are cocondensed with pure $^{14}\text{N}_2$ at 4.2–10°K, the matrix infrared spectrum shown in Figure 6A is obtained. The spectrum shows a group of three lines at 2161.5, 2169.0, and 2179.7 cm^{-1} . In the corresponding matrix Raman experiment, the spectrum shown in Figure 7A

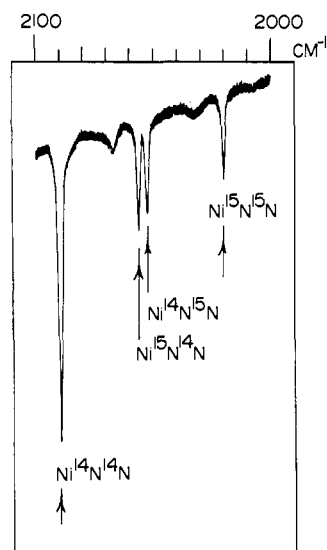


Figure 5. The matrix infrared spectrum of the cocondensation reaction of Ni atoms with a $^{14}\text{N}_2$: $^{14}\text{N}^{15}\text{N}$: $^{15}\text{N}_2$:Ar \cong 3:2:1:4000 mixture at 10°K.

was obtained. Apart from the Raman lines associated with $^{14}\text{N}_2$ and the $^{14}\text{N}^{15}\text{N}$ mixed isotopic molecule present in the low natural abundance (0.3%), three lines were observed in the NN stretching region at 2248, 2179, and 2169 cm^{-1} . Both components of the doublet observed at 2179 and 2169 cm^{-1} were depolarized and were coincident with the two strongest lines observed in the corresponding infrared experiment. However, the Raman line at 2248 cm^{-1} is almost totally polarized.

The matrix infrared and Raman experiments described above were repeated using an approximately equimolar mixture of $^{14}\text{N}_2$ / $^{15}\text{N}_2$. The infrared and Raman spectra so obtained are shown in Figures 6B and 7B, respectively.

Intuitively one expects the Ni nitrogen complex of the highest stoichiometry, that is $\text{Ni}(\text{N}_2)_4$, to be formed in pure nitrogen. Evidently the tetrahedral $\text{Ni}(\text{N}_2)_4$ molecule is sufficiently distorted in the pure N_2 matrix to remove completely the degeneracy of the ir-active T_2 mode. A more accurate analysis which rationalizes this view is given below.

It is interesting to note moreover that Ni in solid CO^6 which is isomorphous with $\alpha\text{-N}_2$ at low temperatures yields a spectrum which is similar to that of Ni in solid N_2 , that is, the degeneracy of the T_2 mode of $\text{Ni}(\text{CO})_4$ is similarly removed.

Frequency Calculations for Isotopically Substituted $\text{Ni}(\text{N}_2)_4$. The frequency and intensity calculations of the $^{14}\text{N}_2$ / $^{15}\text{N}_2$ mixed isotope data are greatly simplified if one assumes that the Cotton-Kraihanzel force field approximation⁹ used for carbonyls may be employed for dinitrogen complexes. Since the data in solid argon for $\text{Ni}(\text{N}_2)_4$ are consistent with a regular tetrahedral molecule, it is a reasonable deduction that the dinitrogen molecule is bonded in an "end on" fashion and that the NiN bond is colinear with the NN bond. In the mixed isotope experiment one has to consider the formation of the five possible complexes listed in Chart I together with the symmetry species of their NN stretching modes and their respective Cotton-Kraihanzel secular equations. A least-squares analysis of the data was performed by adjusting the values of the two pa-

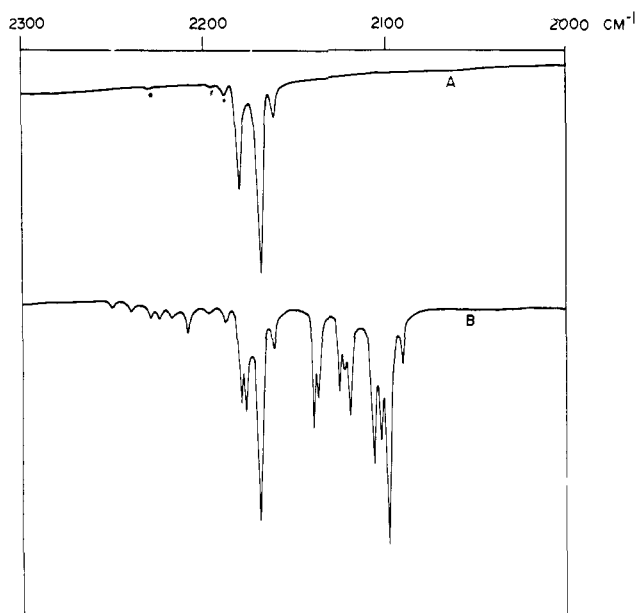


Figure 6. The matrix infrared spectra of the cocondensation reaction of Ni atoms with (A) pure $^{14}\text{N}_2$, (B) an approximately equimolar mixture of $^{14}\text{N}_2$ / $^{15}\text{N}_2$ at 10°K. Note: The very weak lines marked with an asterisk represent aggregate species containing more than one Ni atom, $\text{Ni}_x(\text{N}_2)_y$. This was confirmed by showing that these lines increase in intensity as the rate of Ni atom deposition was increased.

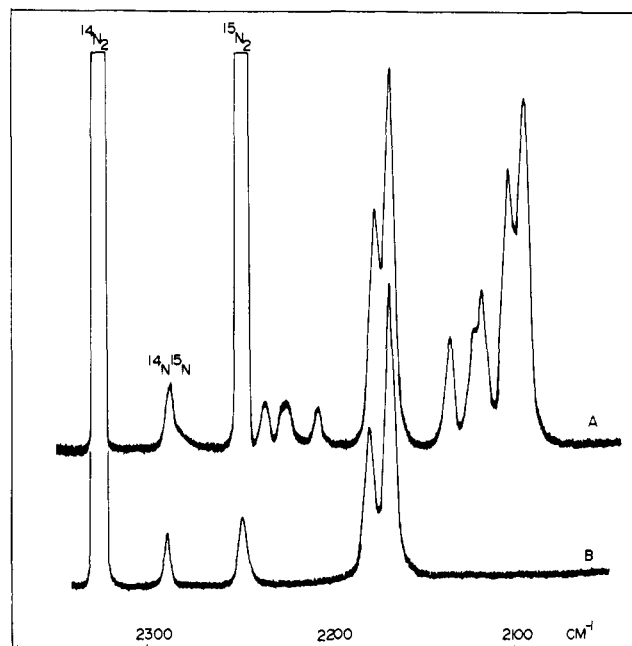


Figure 7. The matrix Raman spectra of the cocondensation reaction of Ni atoms with (B) pure $^{14}\text{N}_2$, (A) an approximately equimolar mixture of $^{14}\text{N}_2$ / $^{15}\text{N}_2$ at 4.2°K.

rameters f_r and f_{rr} to yield the set of frequencies shown in Table II. The agreement between the observed and calculated frequencies is excellent for all NN stretching modes and provides convincing evidence that the T_2 $\text{Ni}(\text{N}_2)_4$ structure is correct for the species of highest stoichiometry in solid argon. $\text{Ni}(\text{N}_2)_4$ is therefore both isoelectronic and isostructural with $\text{Ni}(\text{CO})_4$.

Intensity Calculations. Bos¹⁰ and Haas and Sheline¹¹

(10) G. Bos, *J. Organometal. Chem.*, **10**, 343 (1967).

(11) H. Haas and R. K. Sheline, *J. Chem. Phys.*, **47**, 2996 (1967).

Chart I

	I (T_d)	II (C_{3v})	III (C_{2v})	IV (C_{3v})	V (T_d)
Molecule	Symmetry species		Cotton-Kraihanzel secular equation		
I	T_2	$ f_r - f_{rr} - \frac{\lambda}{\mu_{14}} = 0$			
	A_1	$ f_r + 3f_{rr} - \frac{\lambda}{\mu_{14}} = 0$			
II	E	$ f_r - f_{rr} - \frac{\lambda}{\mu_{14}} = 0$			
	A_1	$\begin{vmatrix} f_r + 2f_{rr} - \frac{\lambda}{\mu_{14}} & \sqrt{3}f_{rr} \\ \sqrt{3}f_{rr} & f_r - \frac{\lambda}{\mu_{15}} \end{vmatrix} = 0$			
III	B_1	$ f_r - f_{rr} - \frac{\lambda}{\mu_{14}} = 0$			
	B_2	$ f_r - f_{rr} - \frac{\lambda}{\mu_{15}} = 0$			
	A_1	$\begin{vmatrix} f_r + f_{rr} - \frac{\lambda}{\mu_{14}} & 2f_{rr} \\ 2f_{rr} & f_r + f_{rr} - \frac{\lambda}{\mu_{15}} \end{vmatrix} = 0$			
IV	E	$ f_r - f_{rr} - \frac{\lambda}{\mu_{15}} = 0$			
	A_1	$\begin{vmatrix} f_r - \frac{\lambda}{\mu_{14}} & \sqrt{3}f_{rr} \\ \sqrt{3}f_{rr} & f_r + 2f_{rr} - \frac{\lambda}{\mu_{15}} \end{vmatrix} = 0$			
V	T_2	$ f_r - f_{rr} - \frac{\lambda}{\mu_{15}} = 0$			
	A_1	$ f_r + 3f_{rr} - \frac{\lambda}{\mu_{15}} = 0$			

Table II. Isotopic Frequency and Infrared Absorption Intensity Calculations for the NN Stretching Modes of $Ni(^{14}N_2)_n(^{15}N_2)_{4-n}$ in Solid Argon^a

Obsd freq	Calcd freq ^b	Obsd inten ^c	Calcd inten	Assignment ^d
2102.0	2101.6	8.15	9.3	$T_2(V)$, $E(IV)$, $B_2(III)$
2112.0	2111.2	2.42	2.1	$A_1(II)$
2123.0	2122.7	2.87	2.7	$A_1(III)$
2138.0	2137.8	1.20	1.7	$A_1(IV)$
2174.0	2175.3	10.00	10.00	$T_2(I)$, $E(II)$, $B_1(III)$
2212.0	2212.2	0.48	0.57	$A_1(IV)$
2228.0	2227.9	0.63	0.69	$A_1(III)$
2240.0	2240.1	0.14	0.14	$A_1(II)$

^a Note that this is the regular tetrahedral form of $Ni(N_2)_4$ (see text). ^b The best fit NN force constants were $f_r = 19.8476$, $f_{rr} = 0.3421$ mdyn/Å. ^c The observed intensities were measured by assuming a triangular contour for the infrared band and using the expression $I = \Delta\nu^{1/2}[1 + \gamma \log \gamma/(1 - \gamma)]$, where $\Delta\nu^{1/2}$ = width of the infrared band at half height γ is the fractional transmittance, and $I = -f \log \gamma$ d ν . ^d See text for notation.

used a relatively simple method for calculating the effect of isotopic substitution on the relative intensities of the infrared bands of metal carbonyls. Despite the fact that the Cotton-Kraihanzel approximation was used and that the method is not rigorously valid in all circumstances, they obtained close agreement between observed and calculated intensities. In neither of the

two papers do the authors indicate in detail how the calculations were performed; consequently we encountered some difficulty in our attempt to carry over these calculations to the nitrogen system. Accordingly we outline the course of one such calculation (that for $Ni(N_2)_4$) in detail.

The integrated intensity of a fundamental infrared band corresponding to normal coordinate Q_k is proportional to the expression

$$I_k = \left(\frac{\partial \mu_x}{\partial Q_k}\right)_0^2 + \left(\frac{\partial \mu_y}{\partial Q_k}\right)_0^2 + \left(\frac{\partial \mu_z}{\partial Q_k}\right)_0^2 = \left(\frac{\partial \mathbf{u}}{\partial Q_k}\right)_0 \left(\frac{\partial \mathbf{u}}{\partial Q_k}\right)_0$$

in which μ_x , μ_y , and μ_z are components of the dipole moment along axes attached to the molecule and Q_k is the normal coordinate of the fundamental mode under discussion. It is more convenient, however, to describe the vibrational modes in terms of their symmetry coordinates. This can be done with the aid of the transformation connecting the normal coordinates with real internal coordinates.¹²

$$S_{k'} = \sum L_{k'k} Q_k$$

the expression for I_k then becomes

$$I_k = \left(\frac{\partial \mathbf{u}}{\partial Q_k}\right)_0 \left(\frac{\partial \mathbf{u}}{\partial Q_k}\right)_0 = \sum_{k'k''} \frac{\partial \mathbf{u}}{\partial S_{k'}} \frac{\partial \mathbf{u}}{\partial S_{k''}} L_{k'k} L_{k''k} \quad (1)$$

The transformation coefficients $L_{kk'}$ are related to the G matrix by

$$\sum_k L_{k'k} L_{k''k} = G_{k'k''} \quad (2)$$

An expression related to the F matrix and λ_k can also be generated (eq 3) where $F_{k'k''}^{-1}$ is an element of the

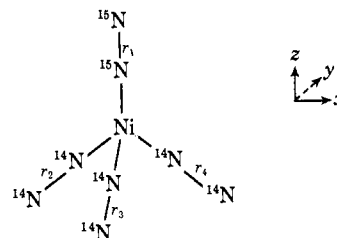
$$\sum_k L_{k'k} \lambda_k^{-1} L_{k''k} = F_{k'k''}^{-1} \quad (3)$$

matrix inverse to the force constant matrix. Thus two intensity sum rules can be formed over all coordinates of a given symmetry species. These can be used to evaluate the intensities of two modes belonging to the same symmetry type which couple. Their application to isotopic molecules is apparent in eq 4 and 5. For

$$\sum_k I_k = \sum_{k'k''} \frac{\partial \mu}{\partial S_{k'}} \frac{\partial \mu}{\partial S_{k''}} G_{k'k''} \quad (4)$$

$$\sum_k \frac{I_k}{\lambda_k} = \sum_{k'k''} \frac{\partial \mu}{\partial S_{k'}} \frac{\partial \mu}{\partial S_{k''}} F_{k'k''}^{-1} \quad (5)$$

example, in $Ni(^{14}N_2)_3(^{15}N_2)$, which has C_{3v} symmetry



(12) E. B. Wilson, J. C. Decius, and P. C. Cross, "Molecular Vibrations," McGraw-Hill, New York, N. Y., 1955.

one can construct the symmetry coordinates of the NN stretching modes using the Cartesian and internal coordinates listed above, as follows.

$$S_1^{A_1} = (1/\sqrt{3})(\Delta r_2 + \Delta r_3 + \Delta r_4)$$

$$S_2^{A_1} = \Delta r_1$$

$$S_3^E = (1/\sqrt{6})(2\Delta r_2 - \Delta r_3 - \Delta r_4)$$

$$S_4^E = (1/\sqrt{2})(\Delta r_3 - \Delta r_4)$$

The components along S_k of the transition dipole moment can then be tabulated together with the G matrix elements.

k	$\partial\mu_x/\partial S_k$	$\partial\mu_y/\partial S_k$	$\partial\mu_z/\partial S_k$	$G_{k'k''}$
1	0	0	-0.58	μ_{14}
2	0	0	1	μ_{15}
3	1.15	0	0	μ_{14}
4	0	1.15	0	μ_{14}

The inverse $F_{k'k''}^{-1}$ matrices are calculated from the $F_{k'k''}$ matrices of the different symmetry species to yield eq 6 and 7. The intensities of the two coupled A_1

$$F^{-1}(A) = \frac{1}{(f_r + 3f_{rr})(f_r - f_{rr})} \begin{vmatrix} f_r & -\sqrt{3}f_{rr} \\ -\sqrt{3}f_{rr} & f_r + 2f_{rr} \end{vmatrix} \quad (6)$$

$$F^{-1}(E) = \frac{1}{(f_r - f_{rr})} \quad (7)$$

modes can then be calculated from the two simultaneous linear eq 4 and 5, while that of the E can be obtained from (4) directly. Applying this method individually to each of the molecules in the isotopic series $\text{Ni}({}^{14}\text{N}_2)_n$ - $({}^{15}\text{N}_2)_{4-n}$ and multiplying the intensity of each by its expected statistical abundance, a set of expected relative intensities may be obtained. Table II summarizes the results of the calculation.

The agreement between measured integrated absorption and calculated intensities is remarkably close and provides further evidence for the formulation of $\text{Ni}(\text{N}_2)_4$ as a regular tetrahedral complex with "end on bonded" dinitrogen.

$\text{Ni}(\text{N}_2)_4$ in Solid Nitrogen. Having established that the highest stoichiometry complex formed in the Ni/N₂ reaction is $\text{Ni}(\text{N}_2)_4$, which in argon matrices is a regular tetrahedral molecule, it is interesting to consider the analogous data in nitrogen matrices. The spectra obtained in argon and nitrogen matrices show gross similarities in terms of the frequencies and intensities of the observed lines. However, the spectra in nitrogen matrices show additional splittings of most of the infrared lines which indicate that the $\text{Ni}(\text{N}_2)_4$ molecule is somehow perturbed from its regular tetrahedral symmetry.

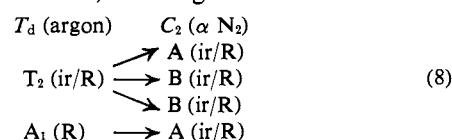
Intuitively one would expect that the perturbation would be caused by the N₂ molecules bonded to the nickel, attempting to take up orientations similar to those that they would have had in the nitrogen lattice. An examination of the reported crystal structure of α -N₂ (Pa 3),¹ which is the stable phase of solid nitrogen below 35°K, is quite informative in terms of the possible sites for the nickel atoms in the lattice. From considerations of the bond length (1.055 Å) and van der Waals radius (1.5 Å) of nitrogen and the atomic radius of nickel (1.3 Å) it appears unlikely that the nickel atom would reside in a tetrahedral site of the nitrogen lattice. The octahedral site, although slightly larger,

does not have N₂ molecules arranged tetrahedrally and need not be considered further.

The nickel atom must then reside in the more spacious substitutional site of the fcc lattice of α -N₂ where there are 12 nearest N₂ neighbors to every nickel atom. Preferential interaction of the nickel atom in the substitutional site with four tetrahedrally disposed nearest neighbor N₂ molecules (it is a matter of conjecture whether a fluxional situation exists) is, then, the most favored scheme for the formation of $\text{Ni}(\text{N}_2)_4$.

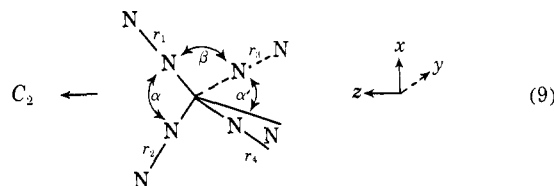
In the unsubstituted N₂ lattice the four tetrahedrally arranged nitrogen molecules about any other N₂ have C₂ symmetry. It is reasonable to assume then that the distortion of the four N₂ molecules "end on bonded" to the Ni which is itself in a substitutional site in the N₂ lattice would be toward C₂. Judging from the proximity of the frequencies of the lines in the undistorted system to those of the distorted system one concludes that the perturbation is slight but large enough, however, to remove the degeneracy of the T₂ mode.

A distortion of the type described would result in the following correlation of the NN stretching modes of $\text{Ni}(\text{N}_2)_4$ (eq 8). That is, the single infrared active ab-



sorption corresponding to the T₂ NN stretching mode of $\text{Ni}(\text{N}_2)_4$ in solid argon (2174 cm⁻¹) splits into three lines (A + 2B) in the C₂ substitutional site of α -N₂.

The perturbation of the molecular symmetry of $\text{Ni}(\text{N}_2)_4$ in solid α -N₂ (usually referred to as "matrix effects") can be placed on a quantitative basis, by computing the frequencies and infrared absorption intensities of a $\text{Ni}(\text{N}_2)_4$ complex with point symmetry C₂ as in (9). The symmetry coordinates for the NN stretch-



ing modes are

$$S_1^A = (1/\sqrt{2})(\Delta r_1 + \Delta r_2)$$

$$S_2^A = (1/\sqrt{2})(\Delta r_3 + \Delta r_4)$$

$$S_3^B = (1/\sqrt{2})(\Delta r_1 - \Delta r_2)$$

$$S_4^B = (1/\sqrt{2})(\Delta r_3 - \Delta r_4)$$

Associating f_{rr} with α , f_{rr}' with α' and f_{rr}'' with β , the secular equations for the A and B symmetry species are (10) and (11). A least-squares analysis of the

$$A \begin{vmatrix} f_r + f_{rr} - \frac{\lambda}{\mu_{14}} & 2f_{rr}'' \\ 2f_{rr}'' & f_r + f_{rr}' - \frac{\lambda}{\mu_{14}} \end{vmatrix} = 0 \quad (10)$$

$$B \begin{vmatrix} f_r - f_{rr} - \frac{\lambda}{\mu_{14}} & 0 \\ 0 & f_r - f_{rr}' - \frac{\lambda}{\mu_{14}} \end{vmatrix} = 0 \quad (11)$$

$\text{Ni}^{14}\text{N}_2/^{15}\text{N}_2$ results was performed in order to obtain the best values of f_r , f_{rr} , f_{rr}' , and f_{rr}'' . Only the thirteen most intense lowest frequency lines were used in the calculation. The analysis yielded the values $f_r = 19.7905$, $f_{rr} = 0.4786$, $f_{rr}' = 0.3741$, and $f_{rr}'' = 0.3157$ mdyn/Å which were used to generate the data tabulated in the "calculated frequency" column of Table III.

Table III. Isotopic Frequency Calculations for the NN Stretching Modes of $\text{Ni}^{(14}\text{N}_2)_n(^{15}\text{N}_2)_{4-n}$ in Solid $\alpha\text{-N}_2$

Obsd freq ^a	Calcd freq	Assignment of modes ^b
2090.0	2091.1	B(5), A(7), B(9)
2097.5	2096.8	B(4), A(8), B(9)
2102.2	2102.2	A(7)
2106.0	2105.9	A(3), A(9)
2119.2	2115.9	A(6)
2122.5	2124.1	B(4)
2125.5	2128.2	B(5)
2137.0	2132.7	A(8)
2139.5	2138.2	A(7)
2161.5	2164.5	B(1), A(2), A(4)
2169.0	2170.4	B(1), A(3), A(5)
2177.0	2176.6	A(2), A(3), A(6)
2179.5	2179.7	A(1)
2209.0	2209.3	A(7)
2217.0	2211.4	A(8)
2225.0	2225.4	A(5), A(6)
2229.0	2229.7	A(4)
2240.0	2239.7	A(2), A(3)
2250.0	2249.1	A(1)
c	2099.3	A(6)
c	2099.9	A(8)
c	2108.5	A(2)
c	2172.8	A(9)

^a The NN stretching force constants for the distorted C_2 form of $\text{Ni}(\text{N}_2)_4$ which gave the best fit were $f_r = 19.7905$, $f_{rr} = 0.4786$, $f_{rr}' = 0.3741$ and $f_{rr}'' = 0.3157$ (see text for notation). ^b See text for notation of C_2 molecule. ^c These frequencies were obscured by other bands or groups of lines. Their exact positions could, therefore, not be determined.

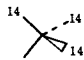
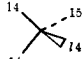
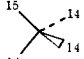
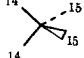
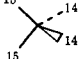
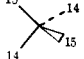
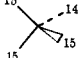
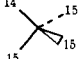
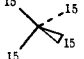
These frequencies are the N-N stretching modes belonging to the nine possible mixed isotopic molecules of the form $\text{Ni}^{(14}\text{N}_2)_n(^{15}\text{N}_2)_{4-n}$ listed in Chart II. The symmetries which the molecules have in solid N_2 are shown beside each as well as the numerical identification used in the assignment column of Table III. The expected infrared intensities of the lines belonging to the (distorted) $\text{Ni}^{(14}\text{N}_2)_4$ were calculated in the manner described above. These are tabulated together with the observed integrated absorptions belonging to that molecule in Table IV.

Both the frequency and intensity calculations show excellent agreement between calculated and measured

Table IV. Frequency and Infrared Absorption Intensity Calculations for the NN Stretching Modes of Distorted $\text{Ni}^{(14}\text{N}_2)_4$ in Solid $\alpha\text{-N}_2$

$\text{Ni}^{(14}\text{N}_2)_4$ (T_d in Ar)		$\text{Ni}^{(14}\text{N}_2)_4$ (C_2 in $^{14}\text{N}_2$)				
	Obsd freq	Calcd freq	Obsd freq	Calcd inten	Obsd inten	
T_2 (ir/R)	B	2162.3	2161.5	2.60	1.60	
	B	2170.0	2169.0	10.00	10.00	
	A	2180.3	2179.7	6.30	4.50	
A_1 (R)	2248	A	2249.0	2248.0	0.008	0.00

Chart II

Molecule	No.	Symmetry
	1	C_2
	2	C_1
	3	C_1
	4	C_2
	5	C_2
	6	C_1
	7	C_1
	8	C_1
	9	C_2

quantities providing convincing evidence in favor of a C_2 substitutional site symmetry for $\text{Ni}(\text{N}_2)_4$ in solid $\alpha\text{-N}_2$.

Force Constant Calculations for $\text{Ni}(\text{N}_2)_3$, $\text{Ni}(\text{N}_2)_2$, and $\text{Ni}(\text{N}_2)$. The lines belonging to the three Ni-nitrogen intermediate molecules $\text{Ni}(\text{N}_2)_x$ where $x = 1, 2, 3$, have been identified previously. Since both infrared and Raman data were obtained for each species, unique values of the N-N bond stretch, and stretch-stretch-interaction force constants are calculable assuming the applicability of the Cotton-Kraihanzel force field simplification. The structures of the three molecules were taken, respectively, to be linear ($C_{\infty v}$), linear ($D_{\infty h}$), and trigonal planar (D_{3h}) based on evidence presented previously. The calculated force constants are compiled in Table V.

Table V. Calculated Cotton-Kraihanzel NN Bond Stretching and Stretch-Stretch Interaction Force Constants^a for $\text{Ni}(\text{N}_2)_n$ (Where $n = 1-4$)

	f_r	f_{rr}
$\text{Ni}(\text{N}_2)_4$	19.85	0.34
$\text{Ni}(\text{N}_2)_3$	19.38	0.59
$\text{Ni}(\text{N}_2)_2$	18.76	0.48
$\text{Ni}(\text{N}_2)$	17.97	

^a Force constant units in mdyn/Å.

$\text{Ni}^{14}\text{N}^{15}\text{N}$ and $\text{Ni}^{15}\text{N}^{14}\text{N}$. The experiment in which Ni atoms were cocondensed into $^{14}\text{N}_2/^{14}\text{N}^{15}\text{N}/^{15}\text{N}_2/\text{Ar}$ in the ratio 1 : 2 : 1 : 4000 deserves special mention in that it provides unique spectroscopic evidence that N_2 bonds "end on" to the nickel. To the extent that one is justified in extrapolating the results of $\text{Ni}(\text{N}_2)_4$ which was shown to have a regular tetrahedral (T_d) symmetry one can state that NiN_2 is a linear ($C_{\infty v}$) rather than a bent triatomic molecule. One can also point out that to date all X-ray studies performed on metal-nitrogen

complexes report only linear metal nitrogen bonding occurs (see, for example, ref 3).

Applying least squares and using well-known equations¹³ the best values of the NiN, NN stretch and NiN, NN stretch-stretch interaction force constants were determined to be 2.38 ± 0.42 , 17.66 ± 0.12 , and 0.26 ± 0.25 mdyn/Å. The "near linear dependence" of the secular equations involved causes the uncertainties in the value of f_{NiN} and $f_{\text{NiN,NN}}$ to be large as indicated.

The 3.8 cm^{-1} split between the two lines belonging to $\text{Ni}^{14}\text{N}^{15}\text{N}$ and $\text{Ni}^{15}\text{N}^{14}\text{N}$ is also noteworthy. Various attempts made primarily by workers interested in the spectra of N_2 chemisorbed on nickel¹⁴ were unsuccessful as a result of the broadness characteristic of the bands of chemisorbed molecules in observing this splitting. Our observation, accordingly, has some bearing on the interpretation of the spectrum of chemisorbed N_2 .

The calculated NN stretch, and stretch-stretch interaction force constants for the four molecules $\text{Ni}(\text{N}_2)_x$ where $x = 1$ to 4 are listed in Table V. The value of f_r is observed to increase monotonically with increasing coordination number in an analogous fashion to that found in binary carbonyls of nickel,¹⁵ strongly suggesting that the simple σ type of bonding from the N_2 to the Ni is supplemented by a degree of $3d\pi-\pi^*$ or $4p\pi-\pi^*$ multiple bonding from the Ni 3d or 4p orbitals to the dinitrogen molecule.

Low Frequency Matrix Infrared and Raman Spectra of $\text{Ni}(\text{N}_2)_4$. Assignment of $\nu_{\text{Ni}-\text{N}_2}$ Stretching Modes. Only in the case of $\text{Ni}(\text{N}_2)_4$ did it prove possible to observe the $\nu_{\text{Ni}-\text{N}_2}$ stretching modes. For the other dinitrogen species in dilute matrices, low frequency skeletal modes were not observed and we are forced to conclude that the metal-nitrogen stretching frequencies have low extinction coefficients and are too weak to observe.

Under ($^{14}\text{N}_2:\text{Ar} = 1:10$) experimental conditions such that the T_2 infrared active $\nu(\text{NN})$ stretching mode of $\text{Ni}(\text{N}_2)_4$ at 2174 cm^{-1} was fully absorbing, a *single* low frequency infrared absorption was observed at 283 cm^{-1} . In an analogous matrix Raman experiment in which the 2174 cm^{-1} band in the Raman was arranged to be full scale, *two* low frequency lines were observed at 303 and 283 cm^{-1} . Matrix Raman depolarization measurements showed that the 303 cm^{-1} line was *totally* polarized while the 283 cm^{-1} line was depolarized.

The low frequency modes observed for $\text{Ni}(\text{N}_2)_4$ are consistent with their assignment to the two expected Ni- N_2 stretching modes of a regular tetrahedral complex. Group theory predicts for the ν_{NN} and ν_{NiN} stretching modes of a tetrahedral molecule

$$\begin{aligned} \Gamma_{\text{NN}} &= A_1(\text{R}) + T_2(\text{ir/R}) \\ &2248 \text{ cm}^{-1} \quad 2174 \text{ cm}^{-1} \\ &(\text{pol } \rho_p \cong 0) \quad (\text{depol } \rho_p \cong 0.75) \\ \Gamma_{\text{NiN}} &= A_1(\text{R}) + T_2(\text{ir/R}) \\ &303 \text{ cm}^{-1} \quad 283 \text{ cm}^{-1} \\ &(\text{pol } \rho_p \cong 0) \quad (\text{depol } \rho_p \cong 0.75) \end{aligned}$$

We note also that the observed depolarization ratios for the totally symmetrical ν_{NN} and ν_{NiN} stretching

(13) G. Herzberg, "Infrared and Raman Spectra of Polyatomic Molecules," Van Nostrand, New York, N. Y., 1945.

(14) R. P. Eischens, *Accounts Chem. Res.*, **5**, 74 (1972), and references therein.

(15) R. L. DeKock, *Inorg. Chem.*, **10**, 1205 (1971).

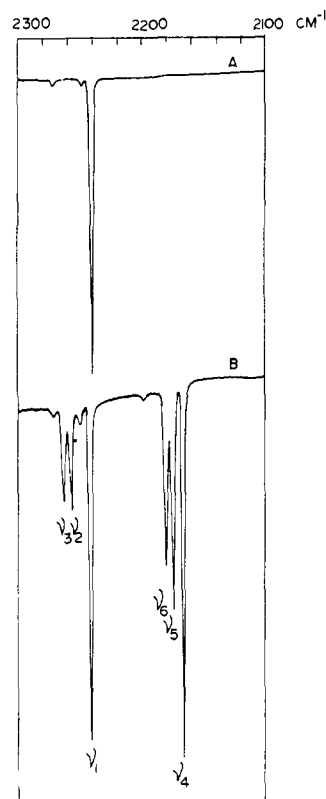


Figure 8. The matrix infrared spectrum of the cocondensation reaction of Pd atoms with (A) pure $^{14}\text{N}_2$, and (B) with an approximately equimolar mixture of $^{14}\text{N}_2/^{15}\text{N}_2$ at 10°K .

modes are approximately zero, which is the calculated value for a molecule having spherical symmetry, that is tetrahedral (T_d) with end-on bonded dinitrogen.

Palladium-Nitrogen System. Tris(dinitrogen)palladium $\text{Pd}(\text{N}_2)_3$, in Solid N_2 . When palladium atoms are cocondensed with $^{14}\text{N}_2$ at 10°K a strong line is observed in the matrix infrared spectrum at 2241 cm^{-1} together with two very weak lines at 2251 and 2274 cm^{-1} (Figure 8A). The corresponding matrix Raman spectrum shows a very strong polarized line at 2274 cm^{-1} (Figures 9A and B).

When the matrix infrared experiment was repeated using an approximately equimolar mixture of $^{14}\text{N}_2$ and $^{15}\text{N}_2$ as matrix gas, the spectrum shown in Figure 8B was observed. The lines observed in pure $^{14}\text{N}_2$ were replaced by *two* groups of lines at 2263.4 , 2256.3 , 2250.8 , and 2241.4 cm^{-1} and at 2182.5 , 2175.6 , and 2166.9 cm^{-1} , respectively with two very weak lines observed at 2273 and 2200 cm^{-1} . In a pure $^{15}\text{N}_2$ matrix one strong band was observed at 2167 cm^{-1} as well as two very weak bands at 2200 and 2175 cm^{-1} . Since only four new lines (there are two overlapping lines at 2175 cm^{-1}) come up when going from $^{14}\text{N}_2/\text{Ar}$ to $^{14}\text{N}_2/^{15}\text{N}_2/\text{Ar}$, the stoichiometry of the most stable Pd/ N_2 complex is not four as in the case of Ni, but three. The four new lines are associated with the species $\text{Pd}(\text{N}_2)_3$ and $\text{Pd}(\text{N}_2)_2$.

The slight infrared activity of the lines at 2251 and 2274 cm^{-1} suggest that, formally, the species $\text{Pd}(\text{N}_2)_3$ does not have a threefold axis of symmetry. Intuitively one suspects that a mechanism similar to that operating in the $\text{Ni}(\text{N}_2)_4/\text{solid } \text{N}_2$ system is responsible for the observed low symmetry of $\text{Pd}(\text{N}_2)_3$ in solid N_2 , and that

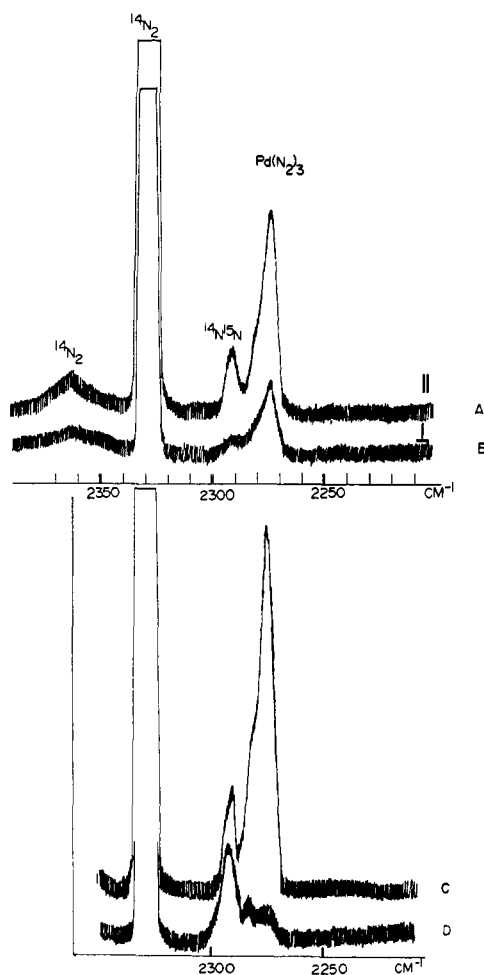


Figure 9. The matrix Raman spectrum of the cocondensation reaction of Pd atoms with pure $^{14}\text{N}_2$ at 4.2°K: (A) parallel polarization, (B) crossed polarization, (C) the same as A but without analyzer, and (D) after diffusion-controlled warm-up at 30°K and re-cooled to 4.2°K.

its symmetry would be higher (D_{3h} or C_{3v}) if the site symmetry perturbations of the N_2 lattice were removed.

Inspection of the $\alpha\text{-N}_2$ crystal structure indicates in fact that of the twelve nearest neighbors about each substitutional site, there are four sets of three nitrogens whose centers of mass are arranged in a trigonal planar fashion. In fact, the site symmetry is C_2 due to the inclination of the N_2 molecules to the plane.

An attempt to obviate the distortion problem by depositing Pd into a 1:1:20 $^{14}\text{N}_2/^{15}\text{N}_2/\text{Ar}$ mixture, then allowing the cocondensate to warm up, was not successful (as it was in the Ni/N_2 system) because, as will be seen below, $\text{Pd}(\text{N}_2)_2$ is not a great deal less stable than $\text{Pd}(\text{N}_2)_3$ and as a consequence the lines of the former persist at all warm-up temperatures.

We propose, therefore, that the Pd nitrogen compound of highest stoichiometry is $\text{Pd}(\text{N}_2)_3$, and that it normally has D_{3h} symmetry which is lowered to C_2 in a pure N_2 matrix; hence the infrared active N-N stretching band belonging to the E' representation is split into an A and a B, which are both infrared active.

Bis(dinitrogen)palladium, $\text{Pd}(\text{N}_2)_2$, and Mono(dinitrogen)palladium, $\text{Pd}(\text{N}_2)$, in Solid Argon. When palladium atoms were cocondensed with dilute $^{14}\text{N}_2/\text{Ar} = 1:10$ mixtures, lines at 2234 cm^{-1} and a doublet at 2215, 2211 cm^{-1} were observed in the matrix infrared

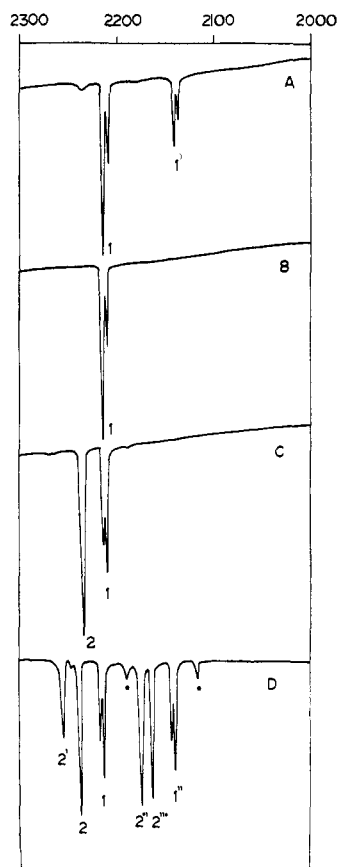


Figure 10. The matrix infrared spectrum of the cocondensation reaction of Pd atoms with (A) a $^{14}\text{N}_2:^{15}\text{N}_2:\text{Ar} = 1:1:2000$ mixture at 10°K, (B) a $^{14}\text{N}_2:\text{Ar} = 1:1000$ mixture, (C) a $^{14}\text{N}_2:\text{Ar} = 1:10$ mixture, (D) a $^{14}\text{N}_2:^{15}\text{N}_2:\text{Ar} = 1:1:20$ mixture.

spectrum (Figure 10C); the corresponding matrix Raman spectrum also displayed two lines, but at 2269 and 2213 cm^{-1} (Figure 11A).

When the infrared experiment was repeated using a $^{14}\text{N}_2:^{15}\text{N}_2:\text{Ar} = 1:1:20$ mixture, the line originally at 2234 cm^{-1} in $^{14}\text{N}_2$ became a quartet (Figure 10D and Table VIII) and that at 2215, 2211 cm^{-1} in $^{14}\text{N}_2$ became a doublet (Figure 10D and Table VIII). This indicates the presence of two species in the matrix, which are satisfactorily assigned to $\text{Pd}(\text{N}_2)_2$ and $\text{Pd}(\text{N}_2)$. The shift to lower frequencies compared to $\text{Pd}(\text{N}_2)_3$ is the expected trend for complexes of lower coordination number than three.

Warm-up experiments on the $^{14}\text{N}_2/^{15}\text{N}_2/\text{Ar} = 1:1:20$ system are shown in Figures 12B-E and clearly show the initial disappearance of $\text{Pd}(\text{N}_2)$ with the simultaneous growth of $\text{Pd}(\text{N}_2)_2$ and finally $\text{Pd}(\text{N}_2)_3$.

A similar growth and decay pattern is observed in the matrix Raman spectrum of the $^{14}\text{N}_2/\text{Ar} = 1:10$ system shown in Figures 11B and C.

The infrared and Raman activities for $\text{Pd}(\text{N}_2)_2$ show that mutual exclusion is operative and that the complex is centrosymmetric. End on bonded dinitrogen is implied in a linear $D_{\infty h}$ structure. When palladium atoms were cocondensed with a very dilute $^{14}\text{N}_2/\text{Ar} = 1:1000$ mixture, only the 2215, 2211 cm^{-1} feature is observed in the matrix infrared spectrum (Figure 10B). This split feature becomes a doublet at 2215, 2211 and 2142 and 2137 cm^{-1} when the experiment was repeated using a $^{14}\text{N}_2/^{15}\text{N}_2/\text{Ar} = 2:1:2000$ (Figure 10A) mixture and confirms the assignment of the 2215, 2211 cm^{-1}

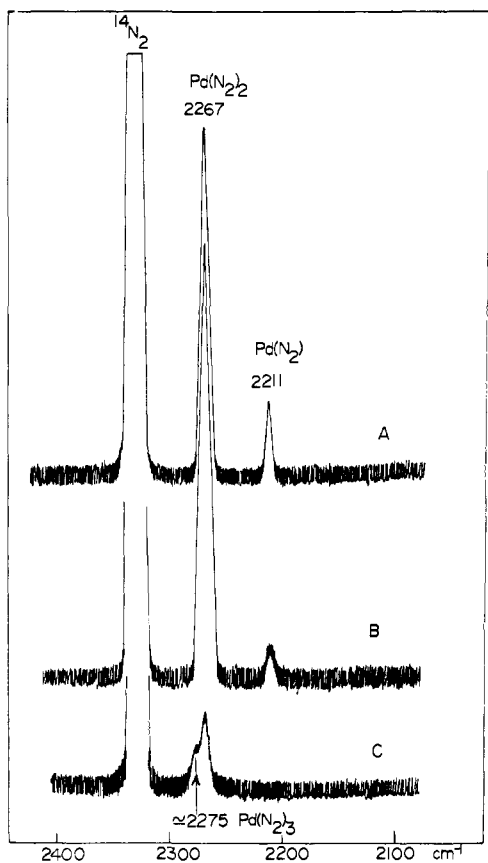


Figure 11. The matrix Raman spectrum of the cocondensation reaction of Pd atoms with a $^{14}\text{N}_2:\text{Ar} = 1:10$ mixture (A) at 4.2°K, (B,C) after successive diffusion-controlled warm-up experiments at 20 and 30°K and recooled to 4.2°K.

doublet to $\text{Pd}(\text{N}_2)$. Further evidence is obtained from the observation of this band (at 2213 cm^{-1} unresolved) in the corresponding matrix Raman experiment (Figure 11A).

The cause of the 2215, 2211 cm^{-1} splitting is not clear. The doublet remains after annealing the N_2/Ar matrices, and may possibly indicate the existence of two slightly different forms of $\text{Pd}(\text{N}_2)$, for example, a linear $C_{\infty v}$ structure and a nonlinear C_s structure.

Force Constant and Intensity Calculations for $\text{Pd}(\text{N}_2)_3$. When the $\text{Pd}/^{14}\text{N}_2$ cocondensate is allowed to warm up, the absorbance of the line at 2251 cm^{-1} grows while that of the 2241 cm^{-1} diminishes in intensity (Figure 13). The two lines (2167, 2175) in the $\text{Pd}/^{14}\text{N}_2$ system behave in an analogous manner. By controlling the Pd deposition rate the line at 2251 cm^{-1} (and its $^{15}\text{N}_2$ analog) can be made vanishingly small. Ordinarily one would explain this behavior by postulating the existence of two nitrogen species in the matrix, one of which grows upon warm up at the expense of the other. In this instance such an explanation is not possible if one considers the following evidence. In the mixed isotope ($^{14}\text{N}_2/^{15}\text{N}_2$) experiment the only lines which grow or decay rapidly are those at 2241, 2251 cm^{-1} and at 2167, 2175 cm^{-1} . In addition when Pd is evaporated into a 1:1 $^{14}\text{N}_2/^{15}\text{N}_2$ matrix at a slow rate (slow enough so that in a $\text{Pd}/^{15}\text{N}_2$ matrix the 2175 cm^{-1} line would not grow), the line at 2175 cm^{-1} nevertheless grows indicating that there are two lines superimposed upon one another at 2175 cm^{-1} . These two

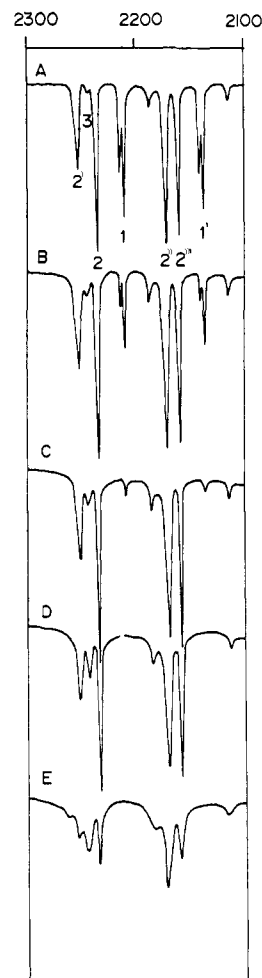


Figure 12. The matrix infrared spectrum of the cocondensation reaction of Pd atoms with (A) a $^{14}\text{N}_2:^{15}\text{N}_2:\text{Ar} = 1:1:20$ mixture at 10°K, (B-E) after successive diffusion-controlled warm-up experiments at 20, 25, 30, and 35°K.

pieces of evidence indicate that the lines at 2263.4, 2256.3, 2182.5, and 2175.6 cm^{-1} belong to the mixed isotopic species whose pure $^{14}\text{N}_2$ analog gives the line at 2241 cm^{-1} . Hence if the line at 2251 cm^{-1} were an independent species it would be a mononitrogen species since it forms a doublet in the $^{14}\text{N}_2/^{15}\text{N}_2$ system. But the mononitrogen species has already been identified in the Pd plus $^{14}\text{N}_2/\text{Ar} = 1:1000$ in which no line is observed at 2251 cm^{-1} . Nor can it be a mononitrogen of an aggregate of Pd since Pd does not diffuse appreciably in a N_2 matrix. One must therefore conclude that the line at 2251 cm^{-1} (and its $^{15}\text{N}_2$ analog at 2175 cm^{-1}) belong to $\text{Pd}(\text{N}_2)_3$ being one of the two components of the E' mode with its degeneracy removed and that the observed growth and decay behavior is an annealing effect. In detail, when first deposited the matrix is irregular; hence the distortion of the $\text{Pd}(\text{N}_2)_3$ species from D_{3h} is at a minimum. When warmed the N_2 matrix anneals thereby increasing the regularity of its crystalline portions, hence increasing the distortion of the $\text{Pd}(\text{N}_2)_3$ from D_{3h} to C_2 , the substitutional site symmetry in αN_2 .

The force constants for the $\text{Pd}(\text{N}_2)_3$ molecule were calculated by applying a least-squares analysis to the observed isotopic frequencies, assuming the Cotton-Kraihanzel approximation and C_2 symmetry for the molecule. Using the notation outlined below f_{rr} was

Table VI. Isotope Frequency and Integrated Infrared Absorption Intensities for $\text{Pd}({}^{14}\text{N}_2)_m({}^{15}\text{N}_2)_{3-m}$ in Solid Nitrogen

Freq notation	Calcd freq	Obsd freq	Calcd inten	Obsd inten	Assignment
Ir ν_1	2242.8	2241.4	10.0	10.0	A(I)
	2250.5	2250.8	10.0	10.0	B(I), B(II)
	2258.2	2256.3	2.9	1.8	A(V)
	2262.8	2263.4	1.3	1.8	A(II)
	2166.7	2166.9	9.3	8.3	A(VI)
	2174.2	2175.5	9.3	8.3	B(VI), B(V)
	2176.4	2175.6	4.6	4.7	A(II)
	2180.8	2182.5	3.0	3.9	A(V)
Raman ν_9	2272.9	2273 ^a			A(I)

^a This frequency and its ${}^{15}\text{N}_2$ counterpart are formally infrared active in the system C_2 . The intensity calculations predict that its intensity will be negligibly small as observed experimentally.

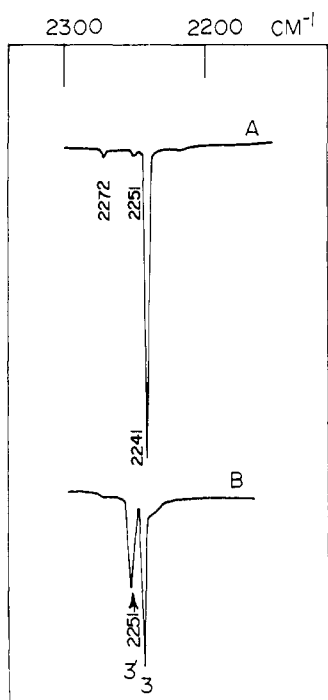
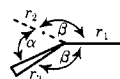


Figure 13. The matrix infrared spectrum of the cocondensation reaction of Pd atoms with ${}^{14}\text{N}_2$ (A) after deposition at 10°K, (B) after diffusion-controlled warm-up at 30°K.



associated with α and $f_{rr'}$ with β . The C_2 axis was taken collinear with r_1 .

Six isotopic molecules are possible in C_2 . These are shown in Chart III together with the symmetry group to which each belongs. The correlation with the four

Chart III

I	$\begin{array}{c} {}^{14} \\ \diagdown \\ {}^{14} \end{array}$	C_2	—	D_{3h}
II	$\begin{array}{c} {}^{14} \\ \diagdown \\ {}^{15} \end{array}$	C_2	\diagup	C_{2v}
III	$\begin{array}{c} {}^{14} \\ \diagdown \\ {}^{15} \end{array}$	C_1	\diagup	C_{2v}
IV	$\begin{array}{c} {}^{15} \\ \diagdown \\ {}^{14} \end{array}$	C_1	\diagup	C_{2v}
V	$\begin{array}{c} {}^{15} \\ \diagdown \\ {}^{15} \end{array}$	C_2	\diagup	C_{2v}
VI	$\begin{array}{c} {}^{15} \\ \diagdown \\ {}^{15} \end{array}$	C_2	—	D_{3h}

D_{3h} molecules from which they are formed is also shown.

Although formally there are six isotopic molecules of the form $\text{Pd}({}^{14}\text{N}_2)_m({}^{15}\text{N}_2)_{3-m}$ the lines in Figure 8B were for the purpose of the force field calculation assigned to the four molecules (I, II, V, VI) closest in symmetry to what they would have had in the D_{3h} system. The calculated and observed frequencies are compared in Table VI.

Using the calculated force constants, the expected frequencies for molecules III and IV were calculated. In all cases these were within *one* wave number of bands present after warm up in the $\text{Pd}/{}^{15}\text{N}_2/{}^{14}\text{N}_2$ spectrum.

The intensity calculation was performed on the basis of a regular trigonal planar rather than a C_2 molecule since it was felt that, *before* warm up, the former structure represented the molecule more accurately than the latter. The results of the calculation are summarized in Table VI.

It should be pointed out, however, that the correct intensity relationship was predicted for the N–N stretching modes of $\text{Pd}({}^{14}\text{N}_2)_3$ as observed after warm up when C_2 symmetry was assumed (Table VII).

Table VII. Integrated Infrared NN Absorptions for $\text{Pd}({}^{14}\text{N}_2)_3$ in Solid N_2 after Warm-up

Freq	Obsd inten	Calcd ^a inten
2241	10	10.0
2251	8	9.9
2274	v.v.w. ^b	0.007

^a Calculation based on a C_2 molecule using the force constants $f_r = 20.9682$, $f_{rr} = 0.09124$, and $f_{rr'} = 0.1955$. ^b This band was present but its absorbance was too weak to measure accurately.

$\text{Pd}(\text{N}_2)_2$ and $\text{Pd}(\text{N}_2)$. The matrix infrared and Raman results indicate that the most probable structures of $\text{Pd}(\text{N}_2)_2$ and $\text{Pd}(\text{N}_2)$ are linear ($D_{\infty h}$) and linear ($C_{\infty v}$), respectively.

The force constants and expected intensities for the two species were calculated from the mixed isotopic spectra in the manner outlined above. Table VIII shows the results of the frequency and intensity calculations. The force constants for the three species $\text{Pd}(\text{N}_2)_n$ ($n = 1, 2, 3$) are shown in Table IX.

One should note that the range of values of f_r among the various Pd–nitrogen species is smaller than in the Ni–nitrogen system indicating that there is less difference in the relative stabilities of the $\text{Pd}(\text{N}_2)_x$ ($x = 1, 2, 3$) than among the various $\text{Ni}(\text{N}_2)_x$ ($x = 1-4$) species. Moreover, the larger values of f_{NN} for the palladium

Table VIII. Isotope Frequency and Integrated Infrared Absorption Intensities for Pd(¹⁴N₂)_x(¹⁵N₂)_{2-x}, Pd(¹⁴N₂), and Pd(¹⁵N₂)

Freq notation	Obsd freq	Calcd freq	Obsd inten	Calcd inten	Assignment
ν_4 (ir)	2252.5	2252.8	4.70	4.9	Pd(¹⁴ N ₂)(¹⁵ N ₂) A ₁
ν_3 (ir)	2234.0	2234.7	10.00	7.7	Pd(¹⁴ N ₂) ₂ Σ_u^+
ν_2 (ir)	2171.5	2170.8	9.15	10.0	Pd(¹⁴ N ₂)(¹⁵ N ₂) A ₁
ν_1 (ir)	2159.5	2159.0	8.81	7.2	Pd(¹⁵ N ₂) ₂ Σ_u^+
(R)	2267.0	2265.1			Pd(¹⁴ N ₂) ₂ Σ_g^+
(ir)	2138.7		4.3	4.7	Pd(¹⁵ N ₂) A ₁
(ir)	2213.0		5.0	5.0	Pd(¹⁴ N ₂) A ₁

Table IX. Calculated Cotton-Kraihanzel NN Bond Stretching and Stretch-Stretch Interaction Force Constants^a for Pd(N₂)_m (Where m = 1-3)

	f_r	f_{rr}	f_{rr}'
Pd(N ₂) ₃	20.97	0.09	0.19
Pd(N ₂) ₂	20.87	0.28	
Pd(N ₂)	20.19		

^a Force constant units in mdyne/Å.

nitrogen compounds relative to those of nickel suggest that the latter are more stable. The values of the N-N stretching frequency in several coordinated dinitrogen complexes (see for example, ref 3) that are stable at room temperature are listed in Table X together with

Table X. Selected Infrared Active N-N Stretching Frequencies for Various Dinitrogen Complexes

Compd	Freq	Ref
Ni(N ₂) ₄	2174	a
Pd(N ₂) ₃	2241	a
Ru(NH ₃) ₃ N ₂ ²⁺	2105-2169 ^b	3
Os(NH ₃) ₃ N ₂ ²⁺	2010-2060 ^b	3
<i>cis</i> -Os(NH ₄) ₄ (N ₂) ₂ ²⁺	2120-2175	3
Ir(PPh ₃) ₂ N ₂ Cl	2190	3

^a Present work. ^b Frequency range obtained with various anions.

the N-N stretching frequencies of Pd(N₂)₃ and Ni(N₂)₄ for the purposes of comparison.

Conclusion

The bonding of the dinitrogen molecule in Ni(N₂)_n and Pd(N₂)_m appears in many respects to be very similar to the coordinated dinitrogen molecule in dinitrogen complexes that are stable at room temperature as well as coordinated CO in carbonyls. We base the conclusion that the dinitrogen ligand in binary nickel and palladium complexes is similar to CO in the binary carbonyls of the same metals on the following points.

(i) Coordinated N₂ gives rise to NN stretching modes shifted to lower frequencies (200-100 cm⁻¹) compared to gaseous N₂.

(ii) A monotonic increase in the NN bond stretching force constants is observed with increasing coordination number.

(iii) The Cotton-Kraihanzel force-field approximation, applied usually to CO in carbonyls, is also successful in predicting NN stretching frequencies in binary dinitrogen complexes.

(iv) Isotope intensity sum rules used previously for calculating the infrared absorption intensities for isotopic carbonyls are also successful in predicting the intensities of infrared active NN stretching modes for N₂ in binary dinitrogen complexes.

(v) Binary Ni(N₂)_n complexes appear to be more stable than the corresponding Pd(N₂)_m complexes (an analogous situation is found for Ni(CO)_n and Pd(CO)_n) as evidenced by the higher NN stretching frequencies for Pd(N₂)_m compared to the corresponding Ni(N₂)_n and by the existence of the higher coordination number complex Ni(N₂)₄ for nickel but only Pd(N₂)₃ for palladium.

(vi) The structures of Ni(N₂)_n and Pd(N₂)_m are similar to those found for the corresponding binary carbonyls. One should perhaps comment on the inability of zero-valent palladium to form a tetradinitrogen complex. Even in pure nitrogen matrices palladium can only be induced to form Pd(N₂)₃. A facile explanation may be made as follows.

If one assumes that the 5p orbitals of Pd are those mainly responsible for the Pd-N₂ π bonding [like the 4p orbitals of nickel in Ni(CO)₄¹⁶], then it seems reasonable that the larger promotion energy requirements for Pd compared to Ni¹⁷ are in part responsible for the 1:3 stoichiometry of the Pd-pure N₂ cocondensation reaction.

Bonding and Frequency Shifts in M(N₂)_n and M(CO)_n Complexes where M = Ni or Pd. Since the preparation of the first stable transition metal complex of molecular nitrogen ³Ru(NH₃)₃(N₂)²⁺, considerable advances have been made in the further synthesis of dinitrogen complexes.¹⁸ Along with the progress in synthetic routes to these complexes a number of direct comparisons between coordinated N₂ and CO were made possible and as a result there has developed some disagreement as to the π acceptor ability of N₂ relative to CO.¹⁸⁻²⁰

The generally accepted and convenient experimental quantity for estimating the π* acceptor property of N₂ or CO from the frequency or bond stretching force constant change on complexation has recently been criticized because of the intuitively disconcerting observation, that for analogous CO and N₂ complexes, Δν_{N₂} is greater than Δν_{CO}. This has been taken to imply that N₂ is a better π acceptor than CO. Mossbauer studies,²¹ on the other hand, demonstrate that CO is an appreciably better σ donor and/or π acceptor than N₂. Although many of these previous investigations have been based on relatively complicated systems the same trends Δν_{N₂} > Δν_{CO} and ΔF_{N₂} > ΔF_{CO} have also been observed

(16) A. F. Schreiner and T. L. Brown, *J. Amer. Chem. Soc.*, **90**, 3366 (1968); K. G. Caulton and R. F. Fenske, *Inorg. Chem.*, **7**, 1273 (1968); K. F. Purcell, *J. Amer. Chem. Soc.*, **91**, 3487 (1969).

(17) C. Moore, NBS Circular 467, Washington, D. C.

(18) J. P. Collman, M. Kubota, F. D. Vastive, J. Y. Sun, and J. W. Kang, *J. Amer. Chem. Soc.*, **90**, 5430 (1968).

(19) K. F. Purcell, *Inorg. Chim. Acta*, **3**, 540 (1969).

(20) K. G. Caulton, R. L. DeKock, and R. F. Fenske, *J. Amer. Chem. Soc.*, **92**, 515 (1970).

(21) G. M. Bancroft, M. J. Mays, and B. E. Prater, *Chem. Commun.*, 585 (1969).

for simple species $\text{NNN}^-/\text{NCO}^-$ and ONN/OCO .¹⁹ The results to date would appear to indicate that the observed frequency and force constant depression order is independent of the substituent, which would imply that the phenomenon stems from differences inherent in the occupied and virtual orbitals of coordinated CO and N_2 .

Since the data for simple binary dinitrogen and carbonyl complexes of Ni and Pd are now available, further insight into the source of the $\Delta\nu_{\text{N}_2}/\Delta\nu_{\text{CO}}$ and $\Delta F_{\text{N}_2}/\Delta F_{\text{CO}}$ orders may be gained.

From an examination of Table XI, it is immediately

Table XI. Comparison of Frequency and Bond Stretching Force Constant Depressions for Binary Dinitrogen and Carbonyl⁶ Complexes of Nickel and Palladium

Coord no., <i>n</i>	$\Delta\nu_{\text{N}_2}$	ΔF_{N_2}	$\Delta\nu_{\text{CO}}$	ΔF_{CO}
Ni				
4	154	2.75	90	1.28
3	191	3.22	117	1.70
2	224	3.84	171	2.07
1	239	4.63	142	2.61
Pd				
4			68	1.16
3	87	1.63	78	1.35
2	94	1.73	88	1.54
1	115	2.41	94	1.73

Mean $[\Delta F_{\text{N}_2}/\Delta F_{\text{CO}}]_{\text{Ni}} = 1.92$; $[\Delta\nu_{\text{N}_2}/\Delta\nu_{\text{CO}}]_{\text{Ni}} = 1.50$
 Mean $[\Delta F_{\text{N}_2}/\Delta F_{\text{CO}}]_{\text{Pd}} = 1.24$; $[\Delta\nu_{\text{N}_2}/\Delta\nu_{\text{CO}}]_{\text{Pd}} = 1.15$

apparent that the order $\Delta\nu_{\text{N}_2} > \Delta\nu_{\text{CO}}$ and $\Delta F_{\text{N}_2} > \Delta F_{\text{CO}}$ observed for other CO and N_2 analogs are also observed for binary CO and N_2 complexes of Ni and Pd. The mean ratio of the frequency shifts for nickel, $(\Delta\nu_{\text{N}_2}/\Delta\nu_{\text{CO}})_{\text{Ni}}$, is 1.50. This value is considerably larger than that for palladium $(\Delta\nu_{\text{N}_2}/\Delta\nu_{\text{CO}})_{\text{Pd}}$, that is, 1.15. Nevertheless, $\Delta\nu_{\text{N}_2} > \Delta\nu_{\text{CO}}$ and $\Delta F_{\text{N}_2} > \Delta F_{\text{CO}}$ still applies.

It has been pointed out that although CO and N_2 have the same total nuclear charge, it is distributed differently in the two molecules.¹⁹ Whereas the π^* (virtual) orbitals in N_2 are evenly distributed between the N atoms, in CO they are more highly concentrated on the C atom. This should give better overlap of metal π orbitals with CO π^* than N_2 π^* which when coupled with the fact, that the CO π^* orbital is calculated at slightly lower energy than that of N_2 , would make CO a better π acceptor. However, computed changes in diatom overlap populations Δn_t for CO and N_2 on coordination which can be broken down into $\sigma(\Delta n_\sigma)$ and $\pi(\Delta n_\pi)$ contributions¹⁹ show that the de-

crease in CO and N_2 π -overlap populations are in the order $\text{N}_2 > \text{CO}$. Thus for a situation in which there is equal population of CO and N_2 π^* orbitals, calculations show the orders $\Pi_a^*(\text{CO}) > \Pi_a^*(\text{N}_2)$ but $\Delta n_\pi(\text{N}_2) > \Delta n_\pi(\text{CO})$.¹⁹ Considerations of this type agree with our experimental findings that $\Delta\nu_{\text{N}_2} > \Delta\nu_{\text{CO}}$ and $\Delta F_{\text{N}_2} > \Delta F_{\text{CO}}$.

However, one can reach essentially the same conclusion by assuming that σ -donation effects alone are the predominant factor. Reference to some recent photoelectron data by Turner, *et al.*,²² is quite illuminating in this respect. It is clear that σ donation alone

Molecule	Electronic state	Vertical IP, eV	ν , cm^{-1}
N_2^+	X $^2\Sigma_g^+$	15.60	2175
N_2^+	A $^2\Pi$	16.98	1850
CO^+	X $^2\Sigma^+$	14.01	2184
CO^+	A $^2\Pi$	16.91	1535

would increase ν_{CO} but decrease ν_{N_2} , and if supplemented by π^* acceptance, the decrease in ν_{N_2} relative to ν_{CO} would be expected to be emphasized further.

If this is indeed the situation, then it is not surprising that the observed $\Delta\nu_{\text{N}_2}$ and ΔF_{N_2} depressions are larger than $\Delta\nu_{\text{CO}}$ and ΔF_{CO} in binary dinitrogen complexes compared to binary carbonyl complexes. In fact one would also expect the σ donation to vary with coordination number which could explain the monotonic variation in NN and CO stretching frequencies. In a situation where σ -donation effects predominate, it is also noteworthy that the larger N_2 and CO frequency and force constant depressions observed for Ni compared to Pd (Table XI) are consistent with the greater electronegativity of Ni ($\chi_{\text{Ni}}^{\text{Ar}} = 1.75$) compared to Pd ($\chi_{\text{Pd}}^{\text{Ar}} = 1.35$).

The discovery of binary dinitrogen complexes of the transition metals and their possible use as intermediates in controlled matrix reactions with other molecules, such as H_2 , will hopefully open up new avenues of investigation to the chemist. Attempts will certainly be made to determine their chemistry and their relationship, if any, to those biological systems which are active in nitrogen fixation.

Acknowledgments. We wish to thank Professors A. D. Allen, A. G. Brook, and E. A. Robinson for financial assistance and continued interest in this work, Mr. Bill Hughes, Mr. Bob Torbet, and Mr. Alex Campbell for technical assistance and the National Research Council of Canada and the Research Corporation for grants in aid of research.

(22) D. W. Turner, "Molecular Photoelectron Spectroscopy," Wiley, New York, N. Y., 1970.